Spherical Harmonic Representation of the Martian Gravity Using a Short-Arc Technique

Edward F. Daniels,* Robert H. Tolson,† and John P. Gapcynski‡
NASA Langley Research Center, Hampton, Va.

Planetary gravity fields are determined primarily from Doppler tracking of orbiting spacecraft, which are typically in high-eccentricity orbits. Thus, the noncentral gravitational components perturb the orbit primarily in the vicinity of periapsis. To find a computationally efficient technique and to reduce the influence of unmodeled forces on the spacecraft, an analysis has been performed of the effectiveness of processing only data in the vicinity of periapsis using multiple short arcs. Although similar short-arc techniques have been utilized for Mascon studies, this analysis is based on a spherical harmonic representation of the gravity field of Mars. Mariner 9 data are processed for the study, using 1-, 2-, 3-, and 4-hr arcs and estimating gravity fields from fourth through seventh degree. The resulting gravity fields are intercompared and also compared with previously published results.

Introduction

PLANETARY orbiting spacecraft are usually in orbits that are of relatively high eccentricity because of propulsive energy considerations. For example, Mariner 9 had an eccentricity e of 0.6, for Viking $e=0.76$, and the Pioneer Venus Orbiter currently is planned with $e=0.84$. Since the forces due to the noncentral components of the gravity field decrease rapidly with the distance from the central body, the gravitational perturbations during such orbits are effective primarily when the spacecraft in the vicinity of periapsis. The principal method for determining planetary gravity fields is by analysis of Doppler tracking data from such orbiting spacecraft. The direct utilization of the precise Doppler data to determine a parameterized representation of the gravity field requires accurate numerical integration of the spacecraft trajectory and a large set of variational equations. For spherical harmonic representations, the integrations typically are performed over a number of orbital periods to emphasize secular and long-period phenomena. Such analyses have been performed by Reasenberg et al.[1] and Lorell et al.[2] on the Mariner 9 data. Reasenberg et al. analyzed data arcs with lengths of both 19 and 38 orbits. They concluded that the shorter arcs produced the most reliable field and that the highest-resolution field that could be estimated was sixth degree. Lorell et al. analyzed data arcs from 6 to 78 orbits in length. They state that eighth or tenth-degree fields may be required for these long arcs to reduce the residuals to below 1 Hz (noise level ≈ 0.01 Hz) and that unmodeled gas leaks may be responsible for the large residuals.

An alternate parameterization of the gravity field, but still using the Doppler data directly, was utilized by Sjogren et al.[3] In this analysis, the anomalistic gravity field was represented by 92 mass points fixed on the surface of Mars. Twenty-eight 2-hr arcs centered on periapsis first were processed to obtain a spacecraft state vector only. The resulting residuals then were processed simultaneously to obtain the masses of the fixed points. This technique is less expensive computationally than the long-arc methods and also reduces the effects of unmodeled nongravitational forces. However, point mass representations require constraints in order to obtain a solution and also are not very amenable to error analysis.

This paper presents a study of the applicability of the multiple short-arc data-analysis technique to determine a spherical harmonic representation of the Mars gravity field. Mariner 9 Doppler data have been analyzed using arc lengths from 1 to 4 hr centered on periapsis and gravity fields through seventh degree. The short arcs provide significant reduction in computer time and in the effects of unmodeled forces on the estimate. On the other hand, short arcs do not permit secular and long-period effects to accumulate. Also, the shorter the arc, the closer the problem approaches the spectroscopic binary star situation, resulting in one state component being nonobservable.

Data Selection

There were three major consideration in the data selection: the data noise, the distribution of data relative to the surface of Mars, and the Earth-spacecraft orbital plane geometry. Mariner 9 provided orbital tracking data from November 1971 through October 1972. During this time, the Earth-Mars distance continually increased, resulting in a general increase in the Doppler noise level. From November 1971 to August 1972 (one month prior to Mars-Sun conjunction), the mean noise level increased from 0.006 Hz (equivalent to about 0.3 mm/sec radial velocity error) to 0.013 Hz.[4] In addition to this general trend, the noise averaged over a station pass varied over a few days' time span by as much as a factor of 5. In early August 1972, the noise level began increasing rapidly to a maximum of about 2.0 Hz at conjunction on Sept. 7. From a data noise standpoint, it was decided that all data earlier than Aug. 1, 1972, would be given equal consideration in the selection, and no attempt would be made to take advantage of the daily variations in noise level.

Resolution of gravity features on the surface of a planet is about equal to the altitude of the spacecraft in the vicinity of periapsis. For Mariner 9, this was 1600 km. Since the Mariner 9 orbit was near the critical inclination, the latitude of periapsis is limited to a narrow band near 20°S lat. Therefore, only a longitudinal variation in distribution of periapsis data is available for selection. To obtain ground tracks with about 1600 km between periapsis longitudes ($\approx 27°$), it was decided to select 16 nearly uniformly spaced orbital passes for analysis. Finally, it is desirable to select spacecraft orbits such that the aerocentric angle between periapsis and the tracking station is minimal. This geometry maximizes the signature in the data of radial acceleration and variations of spacecraft mean motion.

Considering the preceding criteria and the available data, the 16 orbits listed in Table 1 were selected. The longitudes of periapsis could not be selected to be exactly uniform. The

Presented as Paper 76-823 at the AIAA/AAS Astrodynamics Conference, San Diego, Calif., Aug. 18-20, 1976; submitted Oct. 12, 1976; revision received Feb. 14, 1977.

Index category: Spacecraft Signatures and Tracking.

*Aerospace Technologist, Acoustics and Noise Reduction Division.

†Head, Atmospheric Sciences Branch, Atmospheric Environmental Sciences Division. Member AIAA.

‡Aerospace Technologist, Atmospheric Environmental Sciences Division.

Table 1 Geometric characteristics of selected orbits.

Orbit number	Longitude of periapsis, deg	i_{ps}, deg	ϕ, deg
416	6	83	43
420	25	82	44
428	61	83	43
354	80	100	26
360	107	99	27
366	135	97	28
372	164	95	30
376	182	94	31
458	200	73	57
388	237	91	34
468	244	70	60
474	271	69	63
478	290	68	64
404	310	87	39
488	337	66	68
414	357	84	42

maximum longitude between adjacent ground tracks is 37° between orbits 458 and 388, and orbits 388 and 468 are the closest together with a 7° separation. The spacecraft orbit inclination to the plane of the sky (i_{ps}) indicates that the Earth is nearly in the orbital plane for all of these orbits. However, the aerocentric angle between periapsis and the Earth (ϕ) is large during the later orbits. Thus, variations in mean motion will be observed in the Doppler, but only a component ($\cos\phi$) of the radial accelerations at periapsis will be detectable. It should be mentioned that the 16 orbits selected for analysis are among the 28 used by Sjogren et al.[3]

Arc Length and Gravity Field Selection

Spacecraft Forces

Having selected the 16 orbits to be used in the analysis, the next question is how many terms to include in the spherical harmonic expansion of the gravity field and the length of the data arc within each orbit. As the arc length increases, the effect of nongravitational accelerations increases. Reasenberg[1] considers these forces to be a dominant error source in his analysis. For arcs of four orbits or less, the effects are said to be negligible.[5] However, a quantitative analysis[2] by the same authors indicates that these accelerations can bias fourth-degree terms by 100% of their values. The expected level[2] of these unmodeled accelrations is about 10^{-11} km/sec^2. The effect certainly would be nonobservable if the acceleration integrated over the data arc length is significantly less than the data noise. If the integrated acceleration is to be limited to a few tenths of a millimeter per second, the maximum arc lengths then would be a few hours.

For high-eccentricity orbits, the acceleration due to the noncentral components of the gravity field decreases rapidly as the spacecraft recedes from periapsis, the high-degree terms decreasing more rapidly than the low-degree terms. To obtain a quantitative estimate of this effect, consider the radial component of acceleration ($a_{r,nm}$) due to a term (J_{nm}) of degree n and order m. A straightforward calculation shows that the root mean square of $a_{r,nm}$ over the surface of a sphere of radius r

$$\bar{a}_{r,nm} = \left[\frac{1}{4\pi}\int_{4\pi}\int a_{r,nm}^2 \mathrm{d}\sigma\right]^{1/2}$$

is

$$\bar{a}_{r,nm} = (n+1)g_R\,(R/r)^{n+2}\,|J_{nm}| \qquad (1)$$

where $g_R = \mu/R^2$ is the central gravitational acceleration at the reference radius in the gravity field expansion, and J_{nm} is the normalized gravity coefficient. Given errors in normalized gravity coefficients, Eq. (1) also can be used to estimate the corresponding errors in radial accelerations. Kaula[6] gives a rule of thumb for the expected magnitude K_n of normalized gravity coefficients, which can be extrapolated to Mars to yield

$$|J_{nm}| \approx K_n \equiv (5\times 10^{-5})/n^2 \qquad (2)$$

Previous studies of Mars[3] produce gravity field coefficients that are somewhat larger than this rule for low-degree terms but approach this estimate as the degree increases. For convenience, Eq. (2) will be adopted for order-of-magnitude and error-analysis calculations. Combining Eqs. (1) and (2) yields a representative acceleration for any degree term in the gravity field at any distance from Mars. Since the right-hand sides do not depend on the order, the subscript m will be omitted to simplify notation.

To estimate the effect of the gravity terms on the Doppler data, Eq. (1) is integrated over a symmetric interval about periapsis to obtain a velocity change characteristic of an nth-degree term:

$$\Delta V_n \int_{-t}^{t} \bar{a}_{r,n}\mathrm{d}t \qquad (3)$$

The results of this integration are shown in Fig. 1. The Doppler noise level varies between 0.3 and 1.0 m/sec during this phase of the Mariner 9 mission. Eighth- and ninth-degree effects are sufficiently small that they will be difficult to extract from the noise. Thus, the maximum degree considered in the rest of the analysis will be seventh degree.

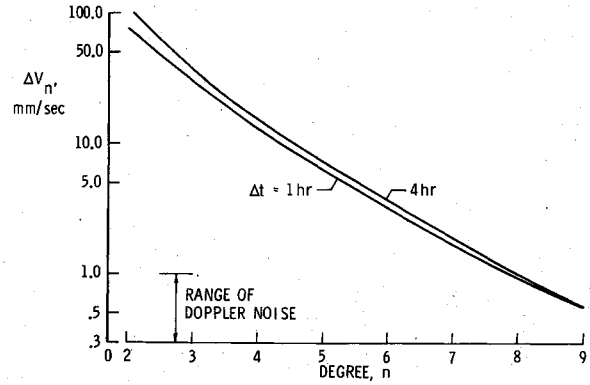

Fig. 1 Integrated rms radial acceleration.

Error Analysis

An error analysis has been performed using the "consider" parameter technique.[7] Data arc lengths of 1, 2, 3, and 4 hr were used to determine gravity fields complete through degrees 4, 5, 6, and 7. A weighted-least-squares (wls) batch algorithm was used. A "consider" covariance was generated, in addition to the covariance based only on data noise. The variances for the "consider" parameters were based on Eq. (2). The parameters considered were all of the higher-degree terms through seventh degree not included in the estimated set. For example, for the case where a fifth-degree field was determined, the sixth and seventh degree terms were the "consider" parameters. No "consider" statistics were generated for the seventh-degree solution.

For each case in which at least terms of two degrees were considered, the lowest degree not included in the solution contributed at least 85% of the final "consider" covariance. Thus, even the statistics associated with the sixth-degree solution should be realistic. The results for this case are shown in Fig. 2. Rather than attempt to show the standard deviations for each gravity coefficient, the degree standard deviations are presented. The degree standard deviation is defined as the root mean square of the normalized standard deviations over

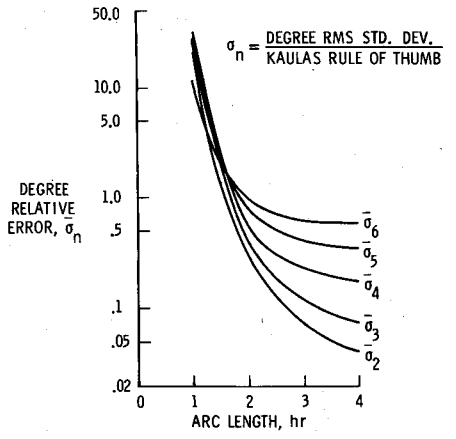

Fig. 2 Degree relative errors for various data arc lengths.

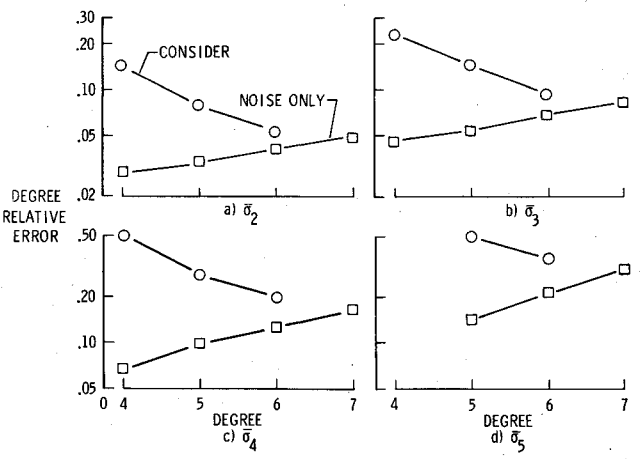

Fig. 3 Degree relative errors for various solution sets.

all $2n+1$ terms of degree n. In addition, the degree standard deviations then are scaled by Eq. (2) to yield the degree relative error, $\bar{\sigma}_n$. Using this ratio reduces the dependence on Eq. (2) in those cases where the "consider" statistics dominate.

Referring to Fig. 2, arcs of 1 hr in length do not provide sufficient strength to yield any meaningful estimates. Two-hour arcs provide only mediocre estimates for even the low-degree terms. There appears to be an advantage to increasing the arc length beyond 4 hr for the second and third-degree terms. On the other hand, 3 hr of data is nearly as effective as 4 hr for the fifth and sixth-degree terms. Based on this result and the possibility of nongravitational force contamination, a 4-hr arc was selected as the basis for the rest of the analysis.

For the fixed set of data now under consideration (16 orbits and 4 hr/orbit), it is possible to determine the optimum solution set by comparing the statistics as the solution set is varied. Figure 3 shows the relative degree errors for second- through fifth-degree terms when solutions are obtained for complete fourth, fifth, sixth, and seventh-degree fields. As expected, the standard deviations, when only data noise is considered, increase as the number of solution parameters increases. The corresponding decrease in "consider" statistics is only slightly due to a reduction in the number of "consider" parameters as the number of solution parameters increases, because, as mentioned earlier, the lowest-degree "consider" parameters contribute about 85% of the total "consider" variances. Even though there are no "consider" statistics for the seventh-degree field, the "consider" relative errors must be larger than the errors when only data noise is included. It appears that, for a seventh-degree solution, the data noise essentially will account for the total standard deviation, a result that also is consistent with Fig. 1. Thus, the optimum solution set appears to be either the sixth- or seventh-degree field.

It is esthetically pleasing if the selected solution set removes most of the signal from the observations, thereby leaving only random noise in the residuals. Figure 4 shows how the rms weighted residual (the function minimized in the wls process) varies with arc length and gravity field solution set. Figure 5 shows one typical arc of residuals resulting from the sixth-degree solution. Both of these figures support the notion that the sixth-degree field has removed most of the signal from the data. However, from Fig. 2 it is seen that the sixth-degree relative error is nearly unity, indicating that there will be little statistical significance to the actual estimates of the sixth-degree terms. But, in contrast, Fig. 3 shows that the relative errors in the second- and third-degree terms have been reduced to more than a factor of 2 by including the sixth-degree terms in the solution.

Comparison of Results

The normalized gravity field coefficients determined by combining sixteen 4-hr arcs of Doppler data are presented in

Table 2 Sixth- and seventh-degree fields from multiple short-arc analysis, $\times 10^7$

		L6		L7				L6		L7	
n	m	C_{nm}	S_{nm}	C_{nm}	S_{nm}	n	m	C_{nm}	S_{nm}	C_{nm}	S_{nm}
2	0	-8773 ±3	-	-8771 ±3	-	6	0	-17 ±8	-	-9 ±7	-
	2	-841 8	505 ±8	-847 6	523 ±8		1	31 7	-21 ±7	53 7	-31 ±6
3	0	-153 3	-	-151 3	-		2	-11 8	55 9	-16 7	26 9
	1	40 3	237 3	46 3	232 3		3	6 8	3 8	17 7	20 7
	2	-158 6	103 5	-171 6	99 5		4	6 8	25 7	8 6	8 6
	3	345 7	263 6	353 1	266 5		5	33 9	19 9	36 7	16 8
4	0	31 4	-	31 4	-		6	28 8	10 9	27 6	-1 9
	1	58 4	29 4	71 4	24 3	7	0	-	-	5 9	-
	2	-17 6	-67 7	-31 6	-82 6		1	-	-	38 8	-12 8
	3	54 8	3 7	72 7	0 6		2	-	-	-6 8	-26 9
	4	3 7	-119 7	-3 6	-125 6		3	-	-	16 8	12 8
5	0	-57 7	-	-49 7	-		4	-	-	20 6	-13 7
	1	8 6	13 5	34 5	8 5		5	-	-	-2 6	-8 7
	2	-59 8	24 9	-70 7	-4 8		6	-	-	14 9	-13 8
	3	22 8	-2 7	42 7	11 6		7	-	-	0 5	-44 5
	4	-59 8	-30 8	-64 6	-38 7						
	5	-42 8	23 6	-48 6	17 5						

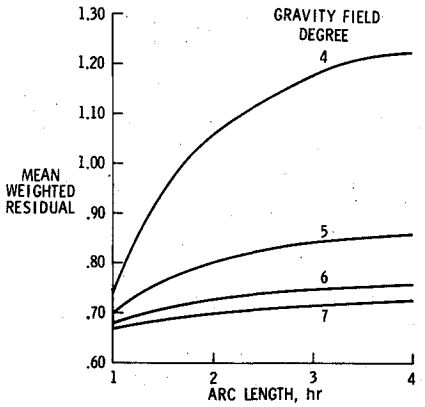

Fig. 4 Rms weighted residual.

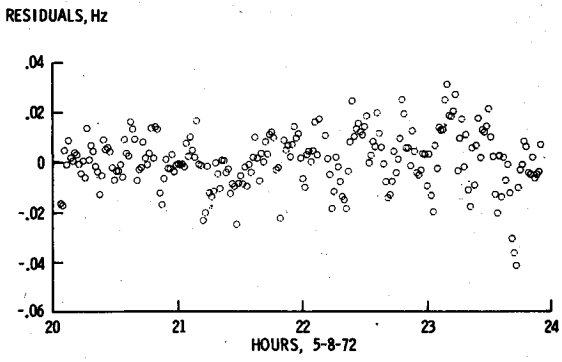

Fig. 5 Residuals for orbit 354, L6 field.

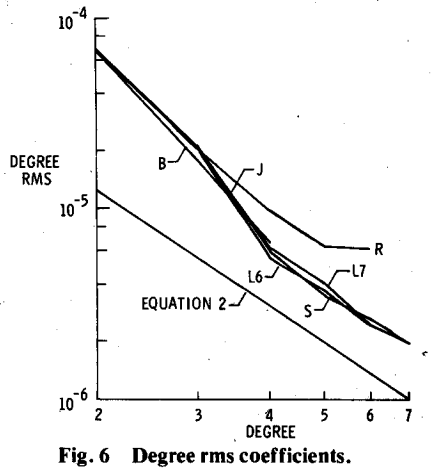

Fig. 6 Degree rms coefficients.

Table 2. Sixth- and seventh-degree solutions are given, since both appeared to have nearly minimal relative errors. The standard deviations for the sixth-degree field are the "consider" statistics discussed earlier. The error estimates for the seventh-degree field are based only on data noise (0.015 Hz). Both fields were obtained without any constraints or conditioning on the estimation algorithm. In fact, the short-arc approach with 4 hr of data appears to be nearly linear in the gravity field parameters, with no serious observability problems. Typically, the gravity field converged after two iterations. One more iteration usually was required to obtain converged state variables. No serious convergence difficulties were encountered until the data arc lengths were reduced to 1 hr. In this case, the observability of the orbital node in the plane of the sky became so poor that convergence aids would be required to obtain a solution.

A number of comparisons have been made between the L6 and L7 results and fields published in Refs. 1, 3, 5, and 8. In order to simplify notation, these latter fields will be identified by the first author's initial (i.e., R—Reasenberg,[1], S—Sjogren,[3] J—Jordan,[5], and B—Born[8]). Note that a corrected value of -0.0005×10^{-4} was used for the coefficient C_{64}, in place of the value listed by Born.[8] A comparison is given in Fig. 6 between $\bar{J}_n$ (the rms over a fixed degree of the normalized coefficients) for each field. The rule of thumb, Eq. (2), also is presented. All of the fields agree well for $n=2$ and 3. Except for R and B, there is also reasonable agreement for $n=4$. The variation of $\bar{J}_n$ for $n=2, 3, 4$, is well represented by a single point mass model. For this model,

$$\bar{J}_n = \left(\frac{m}{M}\right)\frac{1}{2n+1}\left(\frac{r}{R}\right)^n \qquad (n \geq 2)$$

and the best fit occurs for a ratio of point mass to total mass of 3×10^{-3} and a radius of the point mass from the center of Mars of 1200 km ($r/R=0.35$). For $n=4$, it appears that the fields follow a $1/n^2$ rule, but Eq. (2) underestimates by a factor of 2. The three short-arc fields agree well for all values of n.

Another comparison of the field is presented in Table 3. This comparison is made by taking the rms over a fixed degree of the difference between the normalized gravity coefficients from two fields and then dividing by $\bar{J}_n$ from the L7 field. This ratio represents a degree relative error comparable those those in Figs. 2 and 3. The L6 and L7 relative errors compare favorably with the other values in the table; that is, they are not conspicuously larger or smaller. The long-arc fields as a group have larger relative errors than the short-arc fields. This is probably due to aliasing of the coefficients by the unmodeled forces, either the truncated part of the gravity field or the nongravitation forces on the spacecraft. The short-arc fields compare best with the J field. This field "is a composite of many models computed with various filters and different data bases."[5] Therefore, it is not possible to discuss the relative merits of the technique by which this field was derived. Finally, the short-arc fields intercompare very well. In fact, based on the error analysis results presented in Figs. 2 and 3, no better comparison can be expected. This agreement between sample statistics and theoretical statistics lends credance to the assumptions of the error analysis and to the formal statistics quoted in Table 2.

The anomalistic (J_2 deleted) equipotential surface resulting from the L6 field is presented in Fig. 7. Comparing this chart

Table 3 Comparison of degree relative errors

Gravity field		Degree 2	3	4	5	6	7
B	J	.02	.31	1.10	-	-	-
	R	.03	.29	1.19	-	-	-
	S	.05	.32	1.08	-	-	-
	L6	.04	.33	1.05	-	-	-
	L7	.06	.32	1.15	-	-	-
J	R	.02	.17	.91	-	-	-
	S	.03	.07	.18	-	-	-
	L6	.03	.07	.31	-	-	-
	L7	.04	.07	.30	-	-	-
R	S	.02	.18	.92	1.35	2.44	-
	L6	.01	.22	.98	1.63	2.54	-
	L7	.03	.22	.97	1.60	2.54	-
S	L6	.01	.06	.19	.39	.68	-
	L7	.03	.05	.21	.34	.52	.90
L6	L7	.02	.03	.18	.36	.52	-

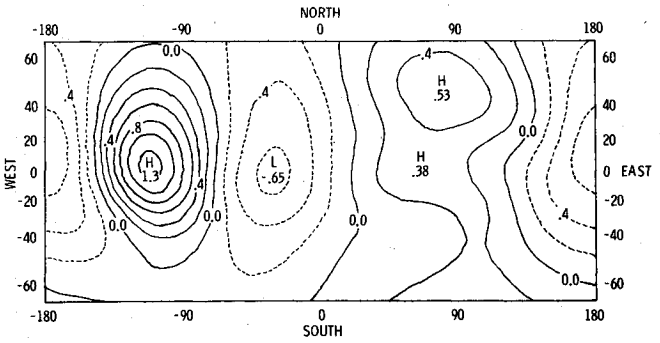

Fig. 7 Equipotential surface height contours for L6 field, km.

Table 4 Rms residuals for independent data sets

	Gravity field					
	B	J	R	S	L6	L7
Mariner 9 Orbit 334	.027	.016	.013	.013	.009	.008
Viking 1 Orbit 29	.053	.013	.023	.011	.0084	.012
Viking 2 Orbit 1	.042	.017	.034	.022	.026	.015

with other published charts, it was found that, between 45°N and 60°S lat, the difference between L6 and S was no more than 60 m. The differences in the polar regions were about 140 m. As expected, larger differences were found when L6 was compared to B (350 m), R (400 m), and J (200 m).

Finally, the gravity fields have been tested with independent data sets. A Mariner 9 orbit was selected (orbit 334) which has a ground track between two of the 16 orbits used in this analysis. In addition, one orbit from each of the Viking missions was used (orbit 29 from VO-1 and orbit 1 from VO-2). The latitude of periapsis was approximately +26° for VO-1 and +50° for VO-2. With the gravity field fixed, a "state-only" solution was obtained for each gravity field using 4 hr of data centered on periapsis. The resulting rms residuals are shown in Table 4. For the Mariner data, the short-arc fields yield a better fit than the long-arc fields. This is also true for the VO-1 data. None of the fields, however, provide a good definition of the gravity field in the vicinity of +50° lat, where the VO-2 periapsis is located. The inclusion of the Viking data should provide significant improvement in all of the models.

Conclusions

The feasibility of using multiple short arcs from highly eccentric orbits to determine a spherical harmonic model of the gravity field of Mars has been demonstrated. Based on the analysis of Mariner 9 data, the short-arc technique yields results equally as valid as any of the published results studied. By proper selection of the arc length, the aliasing due to unmodeled nongravitational forces can be reduced to a negligible level. In addition, through judicous selection of the gravity field solution set, it is possible to limit the effects of the trunctated gravity field to about the same level as the data noise. It therefore is possible to obtain credible formal statistics on the gravity field estimates.

The short-arc technique for spherical harmonic representation of the gravity field also has computational advantages. The method is nearly linear, thereby reducing the number of iterations to obtain a solution. The computation time to process 4 hr of data from either the Mariner 9 or Viking orbits is about half the time of processing a full orbit of data. In addition, the short-arc technique permits greater flexibility in data selection, thereby providing observability and cost benefits. For example, 16 orbits were used in this analysis to obtain longitude coverage with a realistic spacing. To provide complete longitude coverage with a single long arc would require 38 orbits, and the spacing would be more dense than required.

References

[1] Reasenberg, R.C., Shapiro, I.I., and White, R.D., "The Gravity Field of Mars," *Geophysical Research Letters,* Vol. 2, March 1975, pp. 89-92.

[2] Lorell, J. et al., "Gravity Field of Mars from Mariner 9 Tracking Data," *Icarus,* Vol. 18, Feb. 1973, pp. 304-316.

[3] Sjogren, W.L., Lorell, J., Wong, L., and Downs, W., "Mars Gravity Field Based on a Short-Arc Technique," *Journal of Geophysical Research,* Vol. 80, July 1975, pp. 2899-2908.

[4] O'Neill, W.J. et al, "Mariner 9 Navigation," Jet Propulsion Lab., Pasadena, Calif., TR 32-1586, Nov. 1973.

[5] Jordan, J.F. and Lorell, J., "Mariner 9: An Instrument of Dynamical Science," *Icarus,* Vol. 25, May 1975, pp. 146-165.

[6] Kaula, W.M., "The Investigation of the Gravitational Fields of the Moon and Planets with Artificial Satellites," *Advances in Space Science and Technology,* Vol. 5, Academic Press, New York, 1963, pp. 210-226.

[7] Pfeiffer, C.G., Morrison, D.D., Mortensen, R.E., Breakwell, J.V., Berry, W.H., and Merel, M.H., "Sequential Processing Techniques for Trajectory Estimation," NASA CR-1360, 1969.

[8] Born, G.H., "Mars Physical Parameters as Determined from Mariner 9 Observations of the Natural Satellites and Doppler Tracking," *Journal of Geophysical Research,* Vol. 79, Nov. 1974, pp. 4837-4844.